J Geophys (1981) 50: 101–109

Journal of Geophysics

The 3 January 1978 Interplanetary Shock Event as Observed by Energetic Particle, Plasma and Magnetic Field Devices on Board of HELIOS-1, HELIOS-2 and PROGNOZ-6*

A.K. Richter[1], M.I. Verigin[2], V.G. Kurt[3], V.G. Stolpovsky[3], K.I. Gringauz[2], E. Keppler[1], H. Rosenbauer[1], F.M. Neubauer[4], T. Gombosi[5], and A. Somogyi[5]

[1] Max-Planck-Institut für Aeronomie Lindau, Katlenburg-Lindau, Federal Republic of Germany
[2] Space Research Institute, USSR Academy of Sciences, Moscow, USSR
[3] Institute of Nuclear Physics, Moscow State University, Moscow, USSR
[4] Institut für Geophysik und Meteorologie der Technischen Universität, Braunschweig, Federal Republik of Germany
[5] Central Research Institute for Physics, Hungarian Academy of Sciences, Budapest, Hungary

Abstract. We study the different characteristics of the interplanetary medium and of the secondary enhancements in the energetic particle fluxes in the regions before, at and after a flare-generated interplanetary shock wave, as was observed by the solar wind plasma, magnetic field, and energetic particle experiments on board HELIOS-1, HELIOS-2 and PROGNOZ-6 near the Earth's orbit but at different helio-longitudinal positions about 40° apart on 3 January 1978, in the trailing edge of a solar particle event. By intercomparison of the different features in the interplanetary medium, in the energetic particle fluxes, and in the overall structure of the shock wave observed by these three spacecraft, respectively, we find: First, that this shock exhibits the properties of both an *R*- and *F*-type shock event, depending on the point of its observation in space. Second, that the pre-shock intensity enhancements of energetic particles can be explained by a cumulative first-order Fermi acceleration process of successive reflections of these particles at the shock in the entire region between the sun and the orbit of earth. Third, that the post-shock intensity enhancements of energetic particles are due to an acceleration of these particles by the shock wave and/or a trapping of these particles in the downstream region, and a second order Fermi acceleration of these particles by interactions with random Alfvénic and sound wave turbulences. Fourth, that the overall and rapid decrease in the energetic particle intensity observed by all three spacecraft in the downstream region of the shock wave is due to the occurrence of a magnetically closed region (magnetic cloud). Fifth, that the energetic particle enhancements at the shock cannot, at least in case of HELIOS-2, be explained uniquely by the shock drift acceleration mechanism only, as the characteristic angle between the upstream magnetic field direction and the shock surface is not small enough to allow this acceleration mechanism to operate effectively. Thus, highly oblique shocks can also be accompanied by energetic particle intensity increases.

Key words: Particle acceleration – Interplanetary shock waves – Structure of interplanetary shock – Multispacecraft observation

Introduction

Ever since particle and field measurements in interplanetary space with high sensitivity and sufficient high time, energy, and angular resolution have become available, many attempts have been made to study in some detail the frequently observed phenomenon that the flux of charged energetic particles increases in association with propagating interplanetary shocks. Attempts have also been made to compare these observations with current theories on particle acceleration by shock waves (Armstrong et al. 1977, and references therein). These investigations were greatly improved in cases when observations of one and the same event by two or more spacecraft well separated in radial distance from the sun and/or in longitudinal distance were available (Burlaga et al. 1980, and references therein).

Following this latter line of investigation, we shall study in some detail the energetic particle intensity enhancements associated with an interplanetary shock wave observed by the two spaceprobes HELIOS-1 and -2 and the earth-orbiting satellite PROGNOZ-6 on 3 January 1978. Though at that time these three spacecraft were separated by a maximum radial distance of only 0.05 AU and a maximum longitudinal distance of only 40°, HELIOS-1 observed very different features in the fluxes of energetic particles in comparison with HELIOS-2 and PROGNOZ-6, though associated with the same shock wave. In order to understand this phenomenon within the framework of common theories on shock acceleration processes, we will first discuss briefly the overall particle event of 1–4 January 1978, as observed by these three spacecraft and in connection with solar observations. We will then study in greater detail the solar wind plasma and interplanetary magnetic field observations at the time the flare-associated shock wave passes the three spacecraft in question. These observations will provide some insight into the different processes of modulation and acceleration of energetic particles that will occur in the regions before, at and after the shock wave at the positions of these three satellites. Finally, we shall discuss the observed increases of energetic particle fluxes and their variations over these regions, in connection with model calculations on the interaction of these particles with propagating interplanetary shock waves.

The interplanetary plasma, magnetic field and energetic particle data used for this study have been provided in case of HELIOS-1 and -2 by the MPE/MPAE plasma experiment, by the fluxgate magnetometer of the University of Braunschweig, by the MPAE energetic particle spectrometer, and by the energetic particle experiment of the University of Kiel (for further details see the special HELIOS issue of J. Geophys. **42**, 1977), and in case of PROGNOZ-6 by the IKI plasma experiment (Gringauz et al. 1974), by the Izmiran fluxgate magnetometer, and by the energetic particle experiment of the Institute for Nuclear Physics of the Moscow State University, IKI and the Nuclear Research Center of Saclay (Kurt et al. 1979). The solar wind and energetic

* Paper presented at the Workshop on Acceleration of Particles by Shock Waves, October 7–9, 1980, Max-Planck-Institut für Aeronomie Lindau, Katlenburg-Lindau, Federal Republic of Germany

0340-062X/81/0050/0101/$01.80

particle data from IMP-H and -J have been taken from the Solar Geophysical Data, Boulder, U.S.A. Other results used from PROGNOZ-6 observations can be found in the paper by Kurt et al. (1980), which discussed the 1–4 January 1978, event using energetic particle, plasma and magnetic field measurements provided by PROGNOZ-6.

The 1–4 January 1978 Particle Event

At the end of January 1, 1978, the energetic particle detectors on board HELIOS-1, HELIOS-2 and PROGNOZ-6 simultaneously detected an increase in the intensity of energetic protons. In Fig. 1 the overall time-intensity profiles as observed by these spacecraft are shown for protons in the energy range 4–13 MeV (HELIOS-1/-2) and 1.4–5.8 MeV (PROGNOZ-6) together with the times of the occurrence of a flare (*F*) on the sun and the observation of the flare-induced interplanetary shock wave (*S*). The profiles for HELIOS-1 and -2 are taken from the paper by Gombosi et al. (1981). At this time HELIOS-1 is located at 0.95 AU, 169.5° Carrington longitude and 1.7° Carrington latitude, while HELIOS-2 and PROGNOZ-6 are at 0.93 AU, 203.9° and −2.6°, and at 0.98 AU, 209° and −3.1°, respectively. Thus the maximum distances in interplanetary space covered by these three spaceprobes are 0.05 AU in radial direction, about 40° in Carrington longitude and about 4.8° in Carrington latitude. These locations, in the ecliptic plane and relative to the site of the flare on the sun from which this event originated, together with the observed solar wind velocities, are shown in Fig. 2. Though HELIOS-1 and PROGNOZ-6 are separated by only 40° in longitude, the maximum intensity observed by HELIOS-1 is already reached about 6 h after the onset of the event, while PROGNOZ-6 observes a first maximum more than a day later after the onset. This result is at first sight in contradiction to the concept of a fast initial coronal propagation introduced by Reinhard and Wibberenz (1974).

We show in Fig. 3 the time profiles of the solar wind velocities for the same time period, as observed by the three spacecraft in question. In order to obtain the time histories of the solar wind observations at the Earth's orbit as completely as possible, we have added the IMP-J measurements to the PROGNOZ-6 observations by approximating them at those time intervals for which measurements of both spacecraft were available.

The corresponding time scales have been shifted in such a way that the times of the arrival of the flare-associated interplanetary shock wave (*S*) coincides for all three spaceprobes. Note from this figure that during the onset of this event all three satellites are within a rather uniform, low-speed solar wind regime of about 380–430 km/s and, according to the magnetic field observations, of positive interplanetary magnetic field polarity. Taking these velocity values and the actual positions of the spacecraft into account, one can determine their relative locations on the sun by mapping them back along the average interplanetary magnetic field lines (Nolte and Roelof 1973). In Fig. 4 we have marked these three positions on part of the H_α synoptic chart of the Sun (Solar Geophysical Data, Number 407, Part II, 1978). This chart indicates the large-scale polarity regions of the solar magnetic field, the neutral lines, and the active regions. From the H_α solar flare observations one finds that the only active region that is located close enough to the three spacecraft' positions and that, at the same time, was active at the end of 1 January 1978, is located in the plage region 15081. On January 1 at about 21:53 UT, this region produced an H_α flare of importance 2N, which lasted from 21:45–22:16 UT and which was accompanied by solar II, III and IV radio emission,

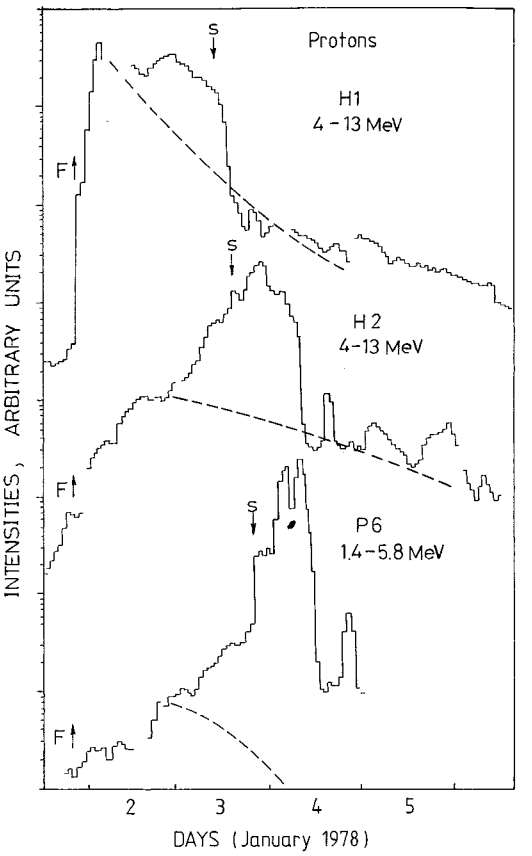

Fig. 1. Time-intensity profiles of the 1 January 1978, particle event occurring at time *F* on the sun, as observed by HELIOS-1 and -2 and PROGNOZ-6 in the energy intervals indicated (one-hour averages). The times of the arrival of the flare generated shock is marked by *S*. The result of Gombosi et al. (1981), who have modelled this event numerically, is shown as *dashed curves*

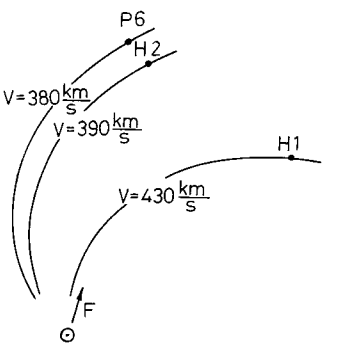

Fig. 2. Positions of HELIOS-1, HELIOS-2 and PROGNOZ-6 in the ecliptic plane and relative to the flare site *F* at the time the flare occurred on the sun. The values of the solar wind velocity, as measured by these three spacecraft at that time, are included

micro wave bursts and X-ray enhancements. Thus we may conclude that both the energetic particle events and the interplanetary shock waves observed by HELIOS-1/-2 and PROGNOZ-6 originated from this region. In addition we find from Fig. 4; first, that the large-scale solar polarity at the positions of the spacecraft coincides with the polarity of the interplanetary magnetic field, as observed by them; second, that at the time the 2N flare occurs HELIOS-1, HELIOS-2 and PROGNOZ-6 are located west relative to this flare, and that HELIOS-1 is well

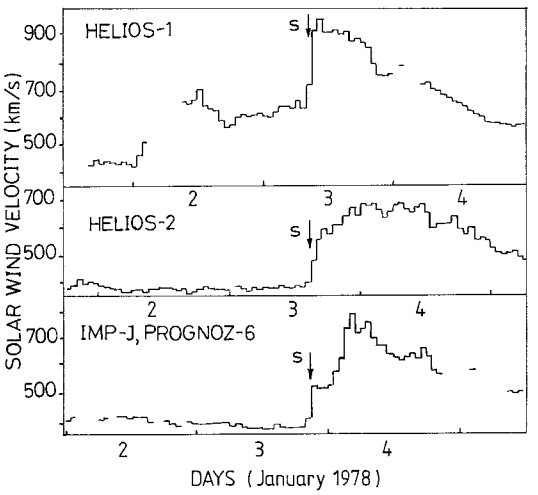

Fig. 3. Time profiles of one-hour averaged solar wind velocity values as observed by HELIOS-1, HELIOS-2 and PROGNOZ-6 during 2–5 January 1978. The passage of the flare generated shock is marked by *S*

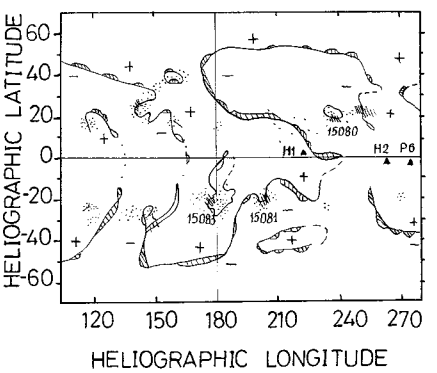

Fig. 4. Part of the H_α synoptic chart of the sun during December 1977–January 1978 showing the large-scale solar magnetic field polarity regions, the neutral lines, and the active regions. The projections of HELIOS-1 and -2 and PROGNOZ-6 at the time of flare onset in region 15081 are shown by *triangles*

separated in longitude from the positions of HELIOS-2 and PROGNOZ-6 and located much closer to the flare-site, even if one takes the approximate error of $\pm 10°$ in Carrington longitude of the Nolte and Roelof technique into account; and third, that by a large, stable neutral line running from the northern solar hemisphere towards the solar equator (about 230° Carrington longitude) the region containing the flare site and the position of HELIOS-1 is separated in some way from the region containing the positions of HELIOS-2 and PROGNOZ-6.. Taking these two latter results and accepted theories on coronal propagation of solar cosmic rays into account, one may well understand why HELIOS-1 observes such a fast increase and large maximum intensity, while HELIOS-2 and PROGNOZ-6 at the same time observe a longer-lasting increase and a smaller first maximum intensity.

At the beginning of 2 January the intensity of the 3–13 MeV protons, observed by HELIOS-1, starts to decrease again, while at HELIOS-2 and PROGNOZ-6 the corresponding intensities are still increasing. Despite the coronal effects mentioned above, we believe that the following interplanetary effect could in addition explain this feature: From Fig. 3 it follows that at this time HELIOS-1, in contrast to HELIOS-2 and PROGNOZ-6,

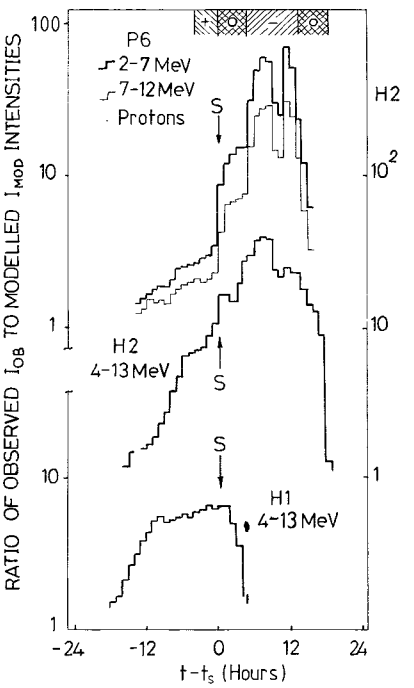

Fig. 5. Time profiles of the ratios of the observed energetic particle intensities to the modelled ones (see Fig. 1). Time in hours refers to the time t_s of the passage of the interplanetary shock *S*. In the upper part the angular direction of the energetic particle fluxes are shown, where + indicates a net streaming away from the sun, – towards the sun, and *o* an isotropic distribution

starts to move into a new and different solar wind regime of high-speed solar wind of more than 600 km/s and of negative interplanetary magnetic field polarity, while HELIOS-2 and PROGNOZ-6 remain in the low-speed solar wind of positive polarity. According to Fig. 4 this could mean that HELIOS-1 becomes disconnected from its previous region on the sun and connected by this high-speed solar wind to the large-scale solar region of negative polarity $+20°$ north of the solar equator. For the following analysis it is important to note that the only active region in this new regime, plage region 15080, is not active between the end of 1 January and about 2:30 UT on 3 January, so that the second maximum observed by HELIOS-1 at the end of 2 January must be associated with the shock wave observed on 3 January, 8:39 UT, rather than with any solar active regions.

Taking coronal and interplanetary propagation effects into account, Gombosi et al. (1981) modelled, using a particular set of coronal and interplanetary propagation parameters, the time-intensity profiles of the 1 January event. Their results are shown as dashed curves in Fig. 1. By comparing the observed and modelled profiles one finds that there is an excess of energetic particles more or less strongly associated with the interplanetary shock waves observed by the three spaceprobes in question. In Fig. 5 we show these excess intensities where we plot the ratios of the observed (I_{ob}) and modelled (I_{mod}) intenstities, respectively. In the following sections we shall concentrate on those parts of the event characterized by the following unique features: An increase of the particle intensity in front of the shock (pre-shock energetic storm particle (ESP) event) observed by all three spacecraft, an increase at the arrival of the shock (shock-spike event) observed by HELIOS-2 and PROGNOZ-6, an increase in the intensity after the shock wave (post-shock ESP event) again observed by HELIOS-2 and PROGNOZ-6,

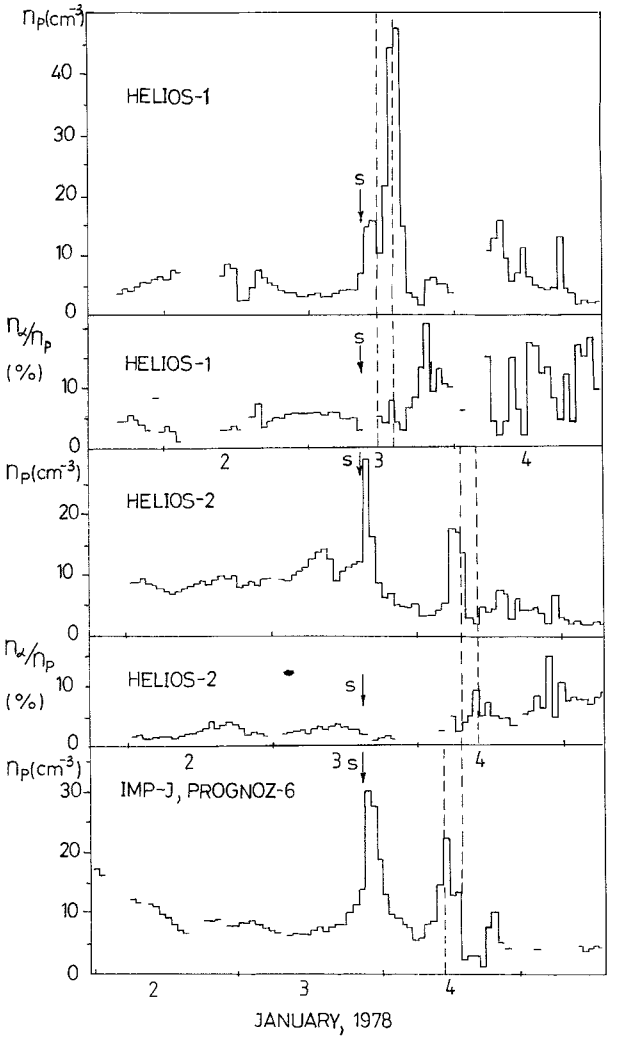

Fig. 6. Time profiles of one-hour averaged values of the solar wind number density N_p (cm^{-3}) and the alpha particle-to-proton ratio $N_\alpha/N_p(\%)$, as observed by HELIOS-1 and -2 and by PROGNOZ-6 and IMP-J. The passage of the shock is indicated by *S*, and the times when the energetic particle intensity drops suddenly (see Fig. 1) by *dashed lines*

and a sharp decrease in the intensity observed by all three space-probes in the downstream region.

The 3 January 1978 Shock Event

The arrival of the interplanetary shock wave associated with the 2N flare on 1 January at 21:53 UT was observed by HELIOS-1, HELIOS-2 and PROGNOZ-6 on 3 January at 8:39 UT, 14:49 UT and 20:48 UT, respectively. According to Figure 3 this shock wave arrived at HELIOS-1 while this spacecraft was located in a high-speed solar wind regime, while it was observed by HELIOS-2 and PROGNOZ-6 at the time when both satellites were still in the low-speed solar wind region. Though HELIOS-1 is located by 0.02 AU further away from the sun than HELIOS-2, the most likely reason for the earlier detection of the shock by HELIOS-1 is most probably due to its propagation through a faster solar wind (Hirshberg et al. 1974).

In order to start with the large-scale features of this shock event we show in Fig. 6 one-hour-averages of the alpha particle-to-proton ratios, $N_\alpha/N_p(\%)$, and of the proton number densities, $N_p(cm^{-3})$, as observed by the plasma experiments on board of HELIOS-1 and 2, PROGNOZ-6 and IMP-J.

Note from this figure that at the shock, *S*, the density N_p increases rapidly to a first maximum in all three cases. In the post-shock regions, however, we find a second and overall maximum increase in N_p directly behind the shock in the case of HELIOS-1, whereas in case of PROGNOZ-6 and HELIOS-2 this second, yet smaller increase in N_p occures about 15–16 h after the shock, respectively. In the case of HELIOS-1 and -2 these second increases in N_p are followed by an increase in the N_α/N_p ratio. In addition these increases are directly accompanied by large directional fluctuations in the interplanetary magnetic field, indicating some kind of 'boundary' between the plasma flow directly behind the shock wave and this alpha particle enriched solar wind region. Analyzing the magnetic field topology in the post-shock regime as observed by HELIOS-2 and IMP for this period of time, Burlaga et al. (1981) found that this 'boundary' is the front part of a magnetic cloud or magnetic loop, in which the observed magnetic field vectors rotate nearly parallel to a plane. The radial dimension of this cloud is approximately 0.5 AU. It should be noted that the occurence of the front boundary of this magnetic cloud is directly associated with the rapid decreases in the intensities of energetic particles as depicted in Fig. 1 and as indicated by dashed lines in Fig. 6. This observation suggests that this cloud is a magnetically closed region preventing energetic particles being behind the shock to propagate further down into this post-shock solar wind region. An alternative suggestion concerning the dynamics of the flow behind the shock waves may be obtained from recent results of magnetohydrodynamic (MHD) models discussing the propagation of shocks in the interplanetary medium: D'Uston et al. (1981) have shown that this flow is often characterized by overexpansion marked by depressed densities and temperatures. Dryer et al. (1980) have demonstrated the closure of the magnetic field in at least one plane across these regions.

It has been proposed by Burlaga et al. (1981) that the shock wave might have been driven by this magnetic cloud closer to the sun, where this cloud may have moved faster. If this would hold, one could argue in view of Fig. 6 that the shock at the position of Helios-1 is still influenced by this magnetic cloud, as it is still attached to the shock (piston-driven shock wave?), whereas at the positions of HELIOS-2 and PROGNOZ-6 the same shock wave is well separated from this magnetic cloud by about 0.15 AU in radial distance and thus no longer influenced by this magnetic loop region (blast-wave type shock?). In order to test this hypothesis we applied the actual solar wind observations in the various regions downstream of the shock to the classification scheme set up by Hundhausen (1972). We find that in the case of HELIOS-1 the shock wave is an *R*-type shock, whereas in case of HELIOS-2 and PROGNOZ-6 it is an *F*-type shock wave. Thus, the 3 January 1978, shock event is another example to be added to the ones given by Ogilvie and Burlaga (1974), that a shock wave can exhibit the properties of blast and piston-driven shock waves at the same time, depending on the longitudinal position of its observation relative to the site of origin on the sun. In turn, we may conclude that the proposed classification of transient shock waves into *R*- and *F*-type shocks cannot be regarded as a unique scheme (see also Rosenau 1979), and it can not therefore be used to draw any conclusions on the origin of these shock waves.

In Fig. 7a the large-scale directional fluctuations perpendicular to the ecliptic plane for both the interplanetary magnetic field (δ_B) and the solar wind velocity (ε_p) vectors are depicted

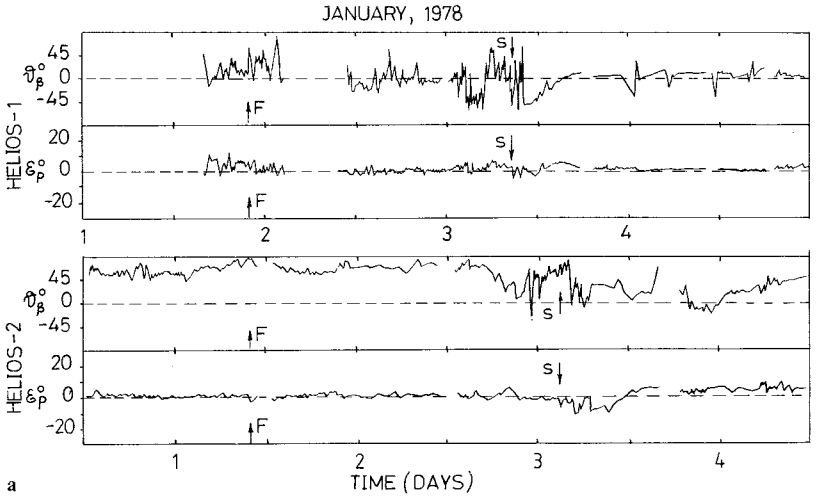

a

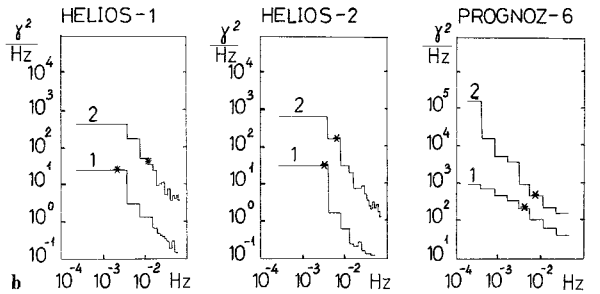

b

Fig. 7. a Time profiles of the fluctuations in the directions of the interplanetary magnetic field (δ°_B) and of the solar wind bulk velocity (ε°_p) out of the ecliptic plane, as observed by HELIOS-1 and -2. The occurrence of the flare is marked by *F*, the passage of the shock by *S*.
b Power spectra of fluctuations in the magnitude of the inter-planetary magnetic field, as observed by HELIOS-1 and -2 and PROGNOZ-6 in the regions before (1) and after (2) the shock wave. Asterisks indicate the doppler-shifted gyrofrequencies of 4 MeV protons in these two regions. The power observed by PROGNOZ-6 is in general higher, as the spacecraft was in the magnetosheath region of the earth at that time

for HELIOS-1 and HELIOS-2. From a systematic survey through more than 9 years of HELIOS' plasma and magnetic field data we found that the level of fluctuations of the angle ε_p clearly indicates the presence of transverse, Alfvénic type of fluctuations in the interplanetary medium. From Fig. 7a we find the following general features for these type of fluctuations: First, they are present in the pre-shock regimes for both HELIOS-1 and HELIOS-2. In case of HELIOS-1, however, they are much more pronounced and larger in amplitude. We found that this holds in general when comparing transverse fluctuations in high-speed solar wind streams with those in low-speed streams. Second, larger-amplitude fluctuations are observed throughout the entire pre-shock region ($\sim$1.5 days since the flare) in the case of HELIOS-1, but for only about 0.7 days before the shock in the case of HELIOS-2. Third, in the post-shock regions one now finds that these transverse fluctuations are of larger amplitude in the case of HELIOS-2 than in the case of HELIOS-1, where they vanish shortly after the shock.

In Fig. 7b the power-spectra of the fluctuations in the magnitude of the interplanetary magnetic field as observed by HELIOS-1 and -2 and PROGNOZ-6 are shown for the pre-shock (1) and the post-shock (2) regions, respecitively. Note that the entire power-spectrum increases in all cases from the pre- to the post-shock region. However, taking the power at the doppler-shifted gyrofrequencies of 4 MeV protons into account (indicated by asterisks in Fig. 7b), we find that this increase in the case of HELIOS-1 is rather small, but nearly an order of magnitude in the case of HELIOS-2.

Finally, taking into account about 5 min averages of plasma and magnetic field parameters for HELIOS-1 and -2, directly in front of and behind the shock waves, and using them to optimize the jump conditions for MHD shocks by a kind of minimum difference technique (Lepping and Argentiero 1971),

Table 1. Some parameters for the shock waves observed by HELIOS-1 and -2

Parameter		HELIOS-1	HELIOS-2
Φ_{ln}		− 76.4°	33.6°
θ_n		− 4.7°	3.7°
$\sphericalangle$ (**r**, **n**)		76.4°	33.8°
$\sphericalangle$ (**B**, **n**)$_1$		130.4°	5.6°
$\sphericalangle$ (**B**, **n**)$_2$		−114.2°	−43.4°
$\sphericalangle$ (**V**, **n**)$_1$		69.3°	3.9°
$\sphericalangle$ (**V**, **n**)$_2$		56.0°	10.4°
$\sphericalangle$ (**B**$_1$, **B**$_2$)		115.4°	48.9°
ΔV_p	(km/s)	157.0	64.1
ΔN_p	(cm^{-3})	4.1	14.7
ΔB	(nT)	5.1	2.7
V_s	(km/s)	406.7	480.2

we can determine all parameters of the shocks and the changes of parameters across the shocks of interest. In Table 1 we have listed some of these values, where **n** denotes the normal of the shock, **r** the radial direction of the sun-spaceprobe line, B the interplanetary magnetic field, V_p the solar wind velocity, N_p its number density, v_s the shock velocity, Δ the changes of solar wind parameters across the shock waves, and the index 1(2) the region before (after) the shock. Note, that for both HELIOS-1 and -2 the angles of the shock normals out of the ecliptic plane (Θ_n) are rather small. In Fig. 8 we show the positions of the shocks of HELIOS-1 and -2, relative to the flare site on the sun, and the directions of their normals and surfaces

together with the overall stream structure and the post-shock boundary, as inferred from Fig. 3 and 6.

The Pre- and Post-Shock ESP Events

It has been shown by Scholer and Morfill (1975) that an increase in the flux of low energetic solar cosmic rays some hours before the arrival of interplanetary shock waves, the so called pre-shock energetic storm particle (ESP) events, can be explained by a gain of energy of these particles due to successive reflections at the moving interplanetary shock front by the first order Fermi process (shock acceleration with scattering in the pre-shock regime). As a result of their numerical model one finds: First, with a reasonable mean free path λ of ~ 0.07 AU for 1 MeV protons in front of the shock their intensity can increase by more than an order of magnitude in the pre-shock regime, followed by a pronounced drop of their intensity about an hour after the shock passage. Second, the number of reflections needed to account for this intensity increase is rather small (2–7 between the sun and 1 AU). Third, the maximum intensity of the ESP event depends roughly on λ in such a way that the smaller λ gets, the larger this intensity enhancement will be.

Comparing these theoretical results with the pre-shock intensity enhancements of the 4–13 MeV protons as observed by HELIOS-1 and -2 (see Fig. 1 and 5) we can develop the following general scenario: Modelling the overall intensity-time profiles of the 1–4 January event (Fig. 1), Gombosi et al. (1981) inferred an averaged interplanetary mean free path of the 4–13 MeV protons between the sun and about 1 AU of $\lambda = 0.10$–0.15 AU. As discussed above this value would be sufficient to account for an intensity enhancement in front of both the HELIOS-1 and -2 shock waves. In order to explain the differences, however, in these two ESP events, namely the location of their maxima relative to the shock fronts and the fact that the maximum intensity observed by HELIOS-2 is much larger than by HELIOS-1, we propose the following explanations: Taking into account the lengths in time (ΔL) of the occurrence of the larger-amplitude transverse fluctuations in the pre-shock regions between the flare onset and the shock arrivals at HELIOS-1 and -2 (Fig. 7a), we find a ratio of roughly ΔL (HELIOS-1)/ΔL(HELIOS-2) ≈ 2.1. On the other hand, taking the distances in time ($\Delta L'$) between the passages of the shock wave and the times when the intensities of the ESP events have decreased by a factor of about $1/e$ of the maximum intensities we find a ratio of roughly $\Delta L'$(HELIOS-1)/$\Delta L'$(HELIOS-2) ≈ 2. Comparing these two ratios, we think that the spread in time of the two pre-shock ESP events is controlled mainly by the spread of the observed larger-amplitude, transverse fluctuations in the interplanetary medium in the pre-shock regions. This would then mean that these local fluctuations have further reduced the mean-free path of the energetic particles in comparison with its averaged value given by Gombosi et al. (1981) at least in case of HELIOS-2.

Using the values given in Table 1, we can determine the anlge Θ between the upstream magnetic field and the shock surface to be $\theta \approx 40°$ and $\theta \approx 84°$ for HELIOS-1 and -2, respectively. As these shocks are oblique, the velocity increment of a particle through a single reflection at the shock will be of the order of $\sim 2\, U_1 \sec\theta$ (Axford 1980, and references herein), where U_1 is the solar wind speed in the pre-shock regime in the rest frame of the shock. Taking the actual values for U_1 and θ into account we find that this increment is higher by a factor of about 4 in the case of HELIOS-2 than in the case of HELIOS-1, or, in other words, the shock at HELIOS-2 is four times more

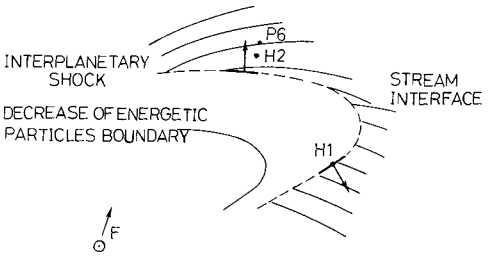

Fig. 8. Sketch of the positions and directions of the shock surfaces and of their normals at the time the interplanetary shock passes HELIOS-1 and -2, together with the overall stream structure of the interplanetary medium and the large-scale post-shock boundary, as inferred from Fig. 6

effective in accelerating particles by reflection than the shock at HELIOS-1. This would then mean, that locally the intensity of reflected particles at a certain energy would be larger at HELIOS-2 than at HELIOS-1, which we indeed observe according to Fig. 5. If this situation holds between the sun and the orbit of the HELIOS spaceprobes, then less than 4 (15) successive interactions of a solar wind particle with the shock front would increase its energy up to 4 MeV in the case of HELIOS-2 (HELIOS-1).

Studying now the post-shock regions, we are going to try to find a number of independent arguments, which could explain why, according to Fig. 1 or 5, the intensity of the 4–13 MeV protons in the post-shock regime of HELIOS-2 is larger than in case of HELIOS-1 by more than an order of magnitude:

– First, applying a very simple model of particle acceleration by plane shocks including convection and diffusion only (snowplough model) the change in the diffusion coefficient κ from the pre- (1) to the post-shock (2) region is given by $\kappa_2/\kappa_1 = (U_2/U_1)^2$, where U is the solar wind speed along the normal to the shock and in the rest frame of the shock (Vasiliev et al. 1980). Taking the actual observations into account, we find that in both cases κ will decrease from the upstream to the downstream region, but that this decrease is larger by a factor of about 2 in the case of HELIOS-2 than in case of HELIOS-1. Thus, particles leaving the shock to go into the post-shock regime can be trapped much more efficiently for HELIOS-2 than for HELIOS-1. According to Scholer and Morfill (1977), who have applied a full propagation model, including diffusion, convection and adiabatic decceleration, this trapping will lead to an increase in the particles' intensity roughly proportional to the decrease in κ.

– Second, still applying the snowplough model it has been shown (Axford, 1980, and references therein) that the increase in the number density behind the shock is directly proportional to the ratio U_1/U_2. This ratio is larger by a factor 1.6 in the case of HELIOS-2 than in the case of HELIOS-1.

– Third, according to Fig. 7a, the amount of large-amplitude transverse fluctuations in the downstream regimes is by far larger in the case of HELIOS-2 than in the case of HELIOS-1. At the same time the level of longitudinal fluctuations at the doppler shifted gyrofrequency of 4 MeV particles is, according to Fig. 7b, again larger by nearly an order of magnitude for HELIOS-2 than for HELIOS-1. These two effects will therefore lead not only to a further decrease of κ_2 for HELIOS-2 and therefore to a further increase of the trapped particle population, but at the same time to an additional turbulent acceleration of particles due to their interaction with random Alfvén and sound waves (second order Fermi mechanism; Toptygin 1980). That this latter effect does indeed occur, can be seen directly

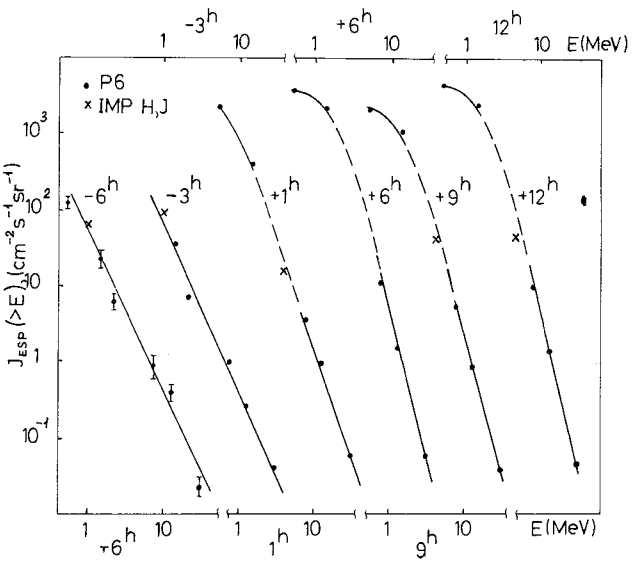

Fig. 9. Spectra of integralintensities vs energy as observed by PROGNOZ-6 and IMP-H, -J from -6 h before to +12 h after the shock

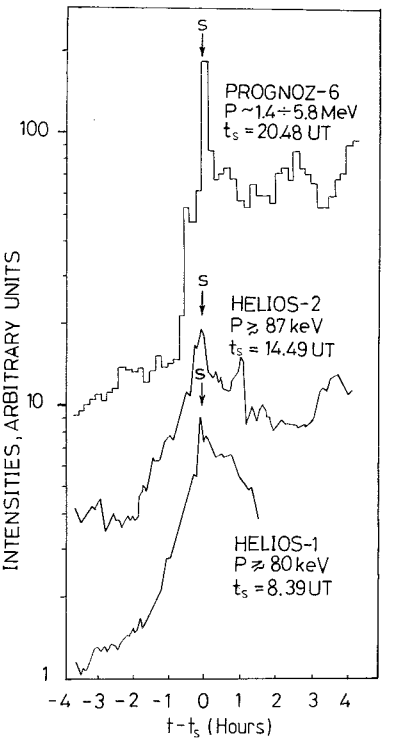

Fig. 10. Time profiles of the low-energetic particle enhancements associated with the passage of the interplanetary shock wave (*S*), as observed by HELIOS-1 and -2 and PROGNOZ-6 at the energies indicated. About ≧5 min averages are used. Time t_s refers to the arrival of the shock

from Fig. 9, where we show the energy spectra of energetic particles ≧0.5 MeV, as observed by PROGNOZ-6 and IMP-J (which are very close to HELIOS-2, as seen from Fig. 8) from −6 h before the shock to +12 h after the shock. From this figure it follows readily that the power-law pre-shock spectrum steepens and is transformed into an exponential spectrum in the post-shock regime in accordance with the results of Toptygin (1980). This is a general feature often observed in cases where particles are accelerated by turbulent wave-fields.

The Shock-Spike Event

In addition to the intensity enhancements of energetic particles in the up- and downstream regions of the interplanetary shock wave, we have already noted from Figure 1 that there is an increase of energetic particle fluxes directly associated with the passage of this shock, the so-called shock-spike event. This situation becomes more obvious if we use a higher time resolution and a lower energy window. For ≧5 min averages, and for 1.4–5.8 MeV protons or ≧80 keV (≧87 keV) ions as observed by PROGNOZ-6 or HELIOS-1 (HELIOS-2), respectively, we can clearly identify this event in Fig. 10.

These observations seem to contradict those accepted theoretical models on the origin of shock-spike events that are based on the shock drift acceleration mechanism (Armstrong et al. 1977; Pesses et al. 1980, and references therein). Within these models the shock itself is regarded as the prime particle accelerator, and the fluctuations of the interplanetary magnetic field in the up- and down-stream regions of the shock are, to first order, ignored. The actual acceleration of low-energy particles to higher energies is then provided by the following, more or less instantaneously operating, non-Fermi mechanism: Positively charged particles interacting with fast-mode shock waves experience a guiding-center drift motion in the shock and are accelerated at the same time by the $\mathbf{V}_p \times \mathbf{B}$ induced electric field being due to the motion of the up- and down-stream solar wind. It has been shown that the efficiency of this mechanism depends crucially on the angle θ between the directions of the pre-shock magnetic field $\mathbf{B}_1$ and the shock surface. For angles $\theta > 10°$ the energy gain should be so small that no noticable shock-spike intensity enhancement should occur. Yet, though $\theta \approx 40°$ and 84° in the case of HELIOS-1 and -2, respectively, we do find rather pronounced intensity increases in association with the shock wave (Fig. 10).

However, as already mentioned by these authors their result, which was obtained for weak, planar and thin shocks without fluctuations in the up- and downstream medium, must be revised if real, observed interplanetary shock waves are considered: The drift of the pre-shock magnetic field lines, around which the particles gyrate, into the shock and the angular change between the upstream and the downstream magnetic field directions may be different to that considered in these model calculations. The shock may be thick and turbulent, and there may be large directional fluctuations of the interplanetary magnetic field just in front of and behind the shock. All these effects could prevent a particle once in the shock from scattering out of this region either into the pre-shock (reflection) or into the post-shock (transmission) regime very easily. Thus, as these processes would increase the possibility of a multiple crossing of the shock, a weaker shock-induced electric field could accelerate these particles to higher energies. Introducing only small angle fluctuations of $\Delta\theta \leqq 10°$ of the pre-shock magnetic field, Armstrong et al. (1977) showed that the maximum energy obtained by particle-shock interaction increases by a factor of roughly 2. In addition, high-frequency directional fluctuations just in front of the shock could temporarily change the angle θ to a value which is favorable for acceleration of particles via the shock drift mechanism.

In Fig. 11 we have plotted the distributions of the angles θ between the directions of the interplanetary magnetic field actually observed by HELIOS-1 and -2 in the pre- and post-shock regions (40.5 s averaged values) and the average directions of the shock surfaces. In addition we have marked the $\theta \leqq 10°$ line

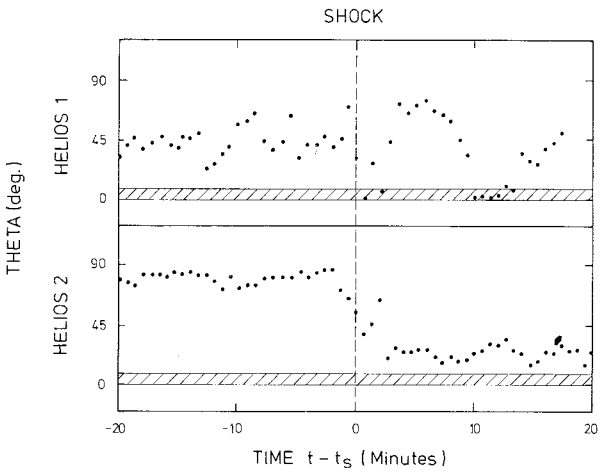

Fig. 11. Distributions of 40.5 s averaged values of the angle θ between the instantaneous direction of the interplanetary magnetic field and the shock surfaces, as observed by HELIOS-1 and -2 about 20 min before and after the passage of the shock wave (*S*). The *shaded regions* for θ are regions for which the acceleration mechanism according to Armstrong et al. (1977) is applicable

of preferred acceleration according to Armstrong et al. (1977). From this figure the following results can be obtained: First, in the regions of a few minutes before and after the shock we find, in the case of both HELIOS-1 and -2, rather large fluctuations in the values of the angle θ. For HELIOS-1 (HELIOS-2) θ ranges from about 30°–65° (55°–87°) in the upstream and from about 0°–75° (20°–64°) in the downstream region, or $\Delta\theta$ from about 10°–25° (3°–30°) or 35°–40° (20°–64°). Second, directly across the shock the angle θ decreases rather abruptly to a value of 0.06° in the case of HELIOS-1. Thus, this effect could explain the occurrence of a shock-spike intensity enhancement for at least the low energetic particles >80 keV. Third, in the case of HELIOS-2, however, the angle θ never decreases below about 35°, though a clear shock-spike intensity enhancement of not only the low ($\geqq$87 keV) but also of the higher energetic particles ($\geqq$4 MeV) is observed. Thus, although still in contradiction with theory we have to conclude that highly oblique shocks can also produce shock-spike events, and that new and refined models are needed to explain such a phenomenon which have to take into account large-amplitude directional fluctuations of the pre- and post-shock magnetic field and therefore enhanced scattering of particles (Fisk and Lee 1980, and references therein).

Conclusions

In this report we have studied the different characteristics of the interplanetary medium and of energetic particle fluxes at different energies in the regions before, at and after one interplanetary shock wave, observed on 3 January 1978 simultaneously by three different spacecraft, near the Earth's orbit but at different longitudinal positions about 40° apart. In order to explain the observed intensity increases of energetic particles in these three regions on the basis of current theories on particle acceleration by propagating shock waves, we found:

First, that really none of them can be explained uniquely on the basis of the shock drift acceleration mechanism only, where the particles interact with the shock, experience a grad **B** drift in the shock, are accelerated at the same time by the shock-induced electric field, and then leave the shock to go into the up- or downstream region, respectively (Armstrong et al. 1977, and references therein). Even taking the observed highly time-resolved fluctuations of the angle θ between the upstream magnetic field direction and the shock surface into account, it has been shown that θ never shows small enough values of below about 5°, that are necessary for this acceleration mechanism to work effectively. Thus, only those models taking also into account the observed large-amplitude fluctuations in direction and in magnitude of the interplanetary magnetic field in the up- and downstream regions may explain the observed features of the energetic particle fluxes in connection with this shock wave (acceleration with scattering).

Second, concentrating on the pre-shock regime we have shown that the shock wave observed by HELIOS-1 and -2 is able to accelerate particles rather effectively by reflection (especially in case of HELIOS-2). As the average mean free path in this region is rather small ($\lambda \leqq 0.08$ AU), and as it may be further reduced locally by the larger-amplitude directional fluctuations observed directly in front of the shock (Fig. 7a), the pre-shock intensity enhancements of energetic particles can be explained by a cumulative first order Fermi process of successive reflections of particles at the shock in the entire region between the sun and the Earth (Scholer and Morfill 1975). This idea is well supported by the following two facts: First, only about four successive reflections over the range of 1 AU would be sufficient to accelerate solar wind particles up to 4 MeV in case of HELIOS-2, and second the widths in time of the intensity enhancements observed by HELIOS-1 and -2 correspond directly with the widths in time of the upstream larger-amplitude directional, Alfvénic type of fluctuations of the interplanetary medium.

Third, going then to the post-shock region and comparing the intensities of energetic particles as observed by HELIOS-1 and -2, we find a huge increase in the case of HELIOS-2 but nearly no effect in the case of HELIOS-1. By inter-comparison of the corresponding plasma and magnetic field observations we can explain this feature by different mechanisms working in the same direction: First, there is a further and larger reduction of the mean free path in the case of HELIOS-2 compared to HELIOS-1, so that transmitted solar flare and/or shock accelerated particles can be trapped more easily in the case of HELIOS-2. This will in general lead to an increase in the particles' intensity (Scholer and Morfill 1977). Second, there are large-amplitude directional fluctuations present in case of HELIOS-2, but almost none in the case of HELIOS-1. Thus in the case of HELIOS-2 an additional first order Fermi acceleration mechanism will work in the downstream medium. Third, there are longitudinal fluctuations present in the post-shock regime, which are more than an order of magnitude more powerful in the case of HELIOS-2 than in the case of HELIOS-1. Thus, a second order Fermi acceleration mechanism will work more effectively in the case of HELIOS-2, due to particle interactions with random Alfvén wave and sound wave turbulences (Toptygin 1980). The bending of the energy spectrum of energetic particles from the post- to the pre-shock region is regarded as evidence that this mechanism works in the case of HELIOS-2 or PROGNOZ-6.

Fourth, in the case of HELIOS-1 and -2 and PROGNOZ-6 there are increases in the intensities of energetic particles directly associated with the passage of the shock wave. In the case of HELIOS-2 and PROGNOZ-6 these increases can also be observed for particles $\geqq$1 MeV. The observation by HELIOS-2 at least stands, at present, in some opposition to the theory on the origin of shock-spike events, if explained by the shock

drift mechanism alone. Thus, we can conclude that highly oblique shocks can also produce shock-spike intensity enhancements of energetic particles, and that new and refined models have to be developed to explain this feature.

Fifth, the classification of interplanetary shock waves into *R*- and *F*-events introduced by Hundhausen (1972), i.e., into events for which the post-shock energy flux of the solar wind rises or falls, is not a 'unique' scheme. In this report we have shown explicitly that one and the same shock wave can be observed as an *R*-event (HELIOS-1) *and* as an *F*-event (HELIOS-2) at the same time. The possibility of this effect was first mentioned by Dryer (1975).

Acknowledgements. Part of this work was done while one of us (A.K.R.) was a guest at the Space Research Institute in Moscow. He wants to thank the director and all colleagues of this institute for their great hospitality. V.G.K. and V.G.S. want to thank Yu. I. Logachev for useful discussions. Finally, all authors want to thank H. Kunow and G. Wibberenz for providing the energetic particle data from HELIOS-1 and -2, as depicted in Figure 1, prior to publication.

References

Armstrong, T.P., Chen, G., Sarris, E.T., Krimigis, S.M.: Acceleration and modulation of electrons and ions by propagating interplanetary shocks, In: Study of Travelling Interplanetary Phenomena. Holland: D. Reidel Publishing Company 1977

Axford, W.I.: The accerlation of galactic cosmic rays. IAU/IUPAP Symposium on Origin of Cosmic Rays, Bologna 1980

Burlaga, L., Lepping, R., Weber, R., Armstrong, T., Goodrich, C., Sullivan, J., Gurnett, D., Kellogg, P., Keppler, E., Mariani, F., Neubauer, F., Rosenbauer, H., Schwenn, R.: Interplanetary particles and fields, November 22 to December 6, 1977: HELIOS, VOYAGER and IMP observations between 0.6 and 1.6 AU. J. Geophys. Res. **85**, 2227–2242, 1980

Burlaga, L., Sittler, E., Mariani, F., Schwenn, R.: Magnetic loop behind an interplanetary shock: VOYAGER, HELIOS, and IMP-8 observations. J Geophys Res **86**, 6673–6684, 1981

Dryer, M.: Interplanetary shock waves: Recent developments. Space Sci. Rev. **17**, 277–325, 1975

Dryer, M., Wu, S.T., Han, S.M.: Two-dimensional, time-dependent MHD simulation of the disturbed solar wind due to representative flare-generated and coronal hole-generated disturbances. Geophysica Int. **19**, 1–15, 1980

D'Uston, C., Dryer, M., Han, S.M., Wu, S.T.: Spatial structure of flare-associated perturbations in the solar wind simulated by a two-dimensional numerical MHD model. J. Geophys. Res. **86**, 525–534, 1981

Fisk, L.A., Lee, M.A.: Shock acceleration of energetic particles in corotating interaction regions in the solar wind. Astrophys. J. **237**, 620–626, 1980

Gombosi, T.I., Green, G., Kecskemety, K., Kunow, H., Kurt, V.G., Logachev, Yu.L., Somogyi, A.J., Stolpovskii, V.G., Wibberenz, G.: Rigidity dependent coronal transport of energetic particles during the January 2–4, 1978 event. 17th Int. Cosmic Ray Conf., Paris, 1981

Gringauz, K.I., Bezrukikh, V.V., Volkov, G.I., Verigin, M.I., Davitaev, L.N., Kopylov, V.F., Musatov, L.S., Shoutchenkow, G.F.: Study of solar plasma near Mars and along the Earth to Mars path by means of charged particle traps aboard the Soviet spacecraft launched in 1971–1973. I. Techniques and devices. Kosmicheskie Issledovaniya **12**, 430–436, 1974

Hirshberg, J., Nakagawa, Y., Wellck, R.E.: Propagation of sudden disturbances through a nonhomogeneous solar wind. J. Geophys. Res. **79**, 3726–3730, 1974

Hundhausen, A.J., Coronal Expansion and Solar Wind. Heidelberg: Springer-Verlag 1972

Kurt, V.G., Logachev, Yu.I., Pisarenko, N.F., Stolpovsky, V.G.: Energetic spectra in solar flare measured by PROGNOZ-6. Izvestiya Academii Nauk SSSR **43**, 3519–3523, 1979

Kurt, V.G., Stolpovskii, V.G., Gombosi, T.I., Kecskemety, K., Somogyi, A.J., Gringauz, K.I., Kotova, G.A., Verigin, M.I., Styazhkin, V.A.: Energetic particle, solar wind plasma and magnetic field measurements on board PROGNOZ-6 during the large scale interplanetary disturbance of January 3–4, 1978, Preprint KFKI-1980-32, Central Research Institute for Physics, Hungarian Academy of Sciences, 1980

Lepping, R.P., Argentiero, P.D.: Single spacecraft method of estimating shock normals. J. Geophys. Res. **76**, 4349–4359, 1971

Nolte, J.T., Roelof, E.C.: Large-scale structure of the interplanetary medium. I. High coronal source longitude of the quiet-time solar wind. Solar Phys. **33**, 241–257, 1973

Ogilvie, K.W., Burlaga, L.: A discussion of interplanetary postshock flows with two examples. J. Geophys. Res. **79**, 2324–2330, 1974

Pesses, M.E., Decker, R.B., Armstrong, T.P.: The acceleration of charged particles in interplanetary shock waves. Johns Hopkins University Preprint JHU/APL 80-10, 1980

Reinhard, R., Wibberenz, G.: Propagation of flare protons in the solar atmosphere. Solar Phys. **36**, 473–494, 1974

Rosenau, P.: Propagation of two-fluid interplanetary shock waves. J. Geophys. Res. **84**, 5897–5906, 1979

Scholer, M., Morfill, G.E.: Simulation of solar flare particle interaction with interplanetary shock waves. Solar Phys. **45**, 227–240, 1975

Scholer, M., Morfill, G.E.: Modulation of energetic solar particle fluxes by interplanetary shock waves. Proceedings of COSPAR Symposium B, AFGL-TR-77-0309, 1977

Toptyghin, I.N.: Acceleration of particles by shocks in a cosmic plasma. Space Sci. Rev. **26**, 157–213, 1980

Vasiljev, V.N., Toptyghin, I.N., Chirkov, A.G.: Particle acceleration at shock waves in turbulent media. Kosmichiskya Issledovania **18**, 556–564, 1980

Received March 6, 1981; Revised version September 29, 1981
Accepted September 30, 1981